A Lumped Thermodynamic Model for Scroll Compressors with Special Attention to the Geometric Characterization during the Discharge Process

Evandro L. L. Pereira
Federal University of Santa Catarina

Cesar J. Deschamps
Federal University of Santa Catarina

A Lumped Thermodynamic Model for Scroll Compressors with Special Attention to the Geometric Characterization during the Discharge Process

Evandro L. L. PEREIRA, Cesar J. DESCHAMPS*

POLO Research Laboratories for Emerging Technologies in Cooling and Thermophysics
Federal University of Santa Catarina
Florianopolis, SC, Brazil
deschamps@polo.ufsc.br

* Corresponding Author

ABSTRACT

A numerical model based on an integral formulation for mass and energy conservation has been developed to simulate the thermodynamic performance of scroll compressors. Internal gas leakages are predicted via a quasi-one-dimensional model that includes viscous and inertial effects. A one-degree of freedom model and a quasi-static model are tested to describe the dynamics of the discharge valve. Unlike most models proposed in the literature, mathematical expressions are written to accurately evaluate both the volume of the compression chamber and the available valve port area during the discharge process. Additionally, a new solution procedure is devised to simplify the code implementation and to improve the convergence of the iterative procedure. The paper analyzes the influence of the aforementioned approaches on the scroll modeling.

1. INTRODUCTION

The scroll compressor is a positive displacement and orbital motion machine, which performs the process of compression by using two identical inter-fitting, spiral-shaped scroll elements, mounted inverted and rotated 180º in relation to each other. When assembled, the flanks of the orbiting and stationary scroll vanes form crescent-shaped pockets. As the scroll orbits, the sealing points (tangent lines) on the vane flanks migrate inward, pushing the pockets toward the involute center. As the pockets move, their volumes are decreased and, consequently, the trapped gas is compressed.

The scroll compressor is well-known for its efficiency in applications that demand high refrigeration capacities. When applied for low refrigeration capacities, it is usually adopted low compression ratio applications, such as air conditioning systems. An advantage inherent to the scroll compressor in comparison to other compression mechanisms is the possibility of not using valves and the longer time available for the suction and discharge processes. Other benefits offered by scroll compressors are the high volumetric efficiency (close to 100% for air conditioning and heat pump applications), low vibration, very quite operation and few moving parts. Among its main sources of thermodynamic irreversibility, pressure equalization at the beginning of the discharge process and internal gas leakages stand out.

The first numerical methodology to simulate scroll compressors was presented by Morishita *et al.* (1984), in which the compression process was modeled via a lumped formulation. Their model served as the basis for the development of several other simulation methodologies (Tojo *et al.*, 1986; Caillat *et al.*, 1988; Nieter, 1988; Yanagisawa *et al.*, 1990; Suefuji *et al.*, 1992; Chen *et al.*, 2002). Among all models that adopt a lumped formulation, the one described by Chen *et al.* (2002) can presently be considered the most comprehensive. In such models, different approaches are employed to predict the gas leakage, becoming clear the existence of some uncertainty about the best practice. However, the modeling of leakage with reference to an isentropic flow in nozzles seems to be the most widespread technique, with viscous effects being included by means of contraction flow factors.

This paper presents a numerical model developed to simulate the thermodynamic performance of scroll compressors. The mass and energy conservation equations are solved through a lumped formulation and a real gas equation of state is adopted via libraries provided by REFPROP (NIST, 2008). Mass flow rates in the suction and discharge processes, as well as leakage in flank clearances, are calculated from relationships based on the isentropic flow condition. However, a quasi-1D model that includes viscous and inertial effects is used to predict the gas flow through the top clearance. A one-degree of freedom model is used to describe the discharge valve dynamics. Through a new solution procedure, the model is applied to investigate the influence of different modeling approaches on prediction for the compressor thermodynamic performance.

2. MATHEMATICAL MODEL

2.1 Geometrical Considerations

The shape of the scroll here considered is an involute of a circle. The scroll is consequently defined by two involutes that are developed around a common basic circle of radius a and that are offset by a constant distance r_o. From the definition of involute, the distance L of one point on the involute to its tangent point on the base circle must satisfy the following mathematical relationship:

$$\frac{\partial L(\varphi)}{\partial \varphi} = a \tag{1}$$

where φ is the involute angle. For a scroll with N compression chambers, φ varies from the involute initial angle φ_s to the involute final angle φ_e ($\varphi_e = 2\pi N + \pi/2$). Therefore, by integrating Eq. (1) and assuming that a is a constant, the equations describing the pair of involutes in polar coordinates can be obtained (Chen *et al.*, 2002). From these relationships, the scroll vane thickness t, the orbiting radius of the rotating scroll r_o and the displacement volume V_{sw} can be written as follows:

$$t = 2a\varphi_i \tag{2}$$

$$r_o = a\pi - t \tag{3}$$

$$V_{sw} = 4\pi^2 a(\pi a - t)(2N - 1)h \tag{4}$$

where h is the scroll vane height.

The central region of the scroll can be designed with different geometric shapes. In the present study, a perfect mesh profile (PMP) in the central region is constructed from the geometric and mathematical description given by Zhenquan *et al*. (1992), which is a function of a modified angle γ, chosen by the designer, and an angle β that must satisfy the following relationship:

$$\mathrm{ctg}\,\beta + 2\beta = \pi + \gamma \tag{5}$$

Therefore, the discharge angle θ_d and the maximum discharge radius r_d for a circular port are calculated by:

$$\theta_d = 2\pi N - \gamma \tag{6}$$

$$r_d = \frac{a}{\mathrm{sen}(2\beta)} - \frac{r_o}{2} \tag{7}$$

Such profiles allow higher compression ratios as well as longer time intervals for the discharge process; i.e. one complete revolution of the crankshaft for $\gamma = 0$.

The expressions adopted to evaluate the top leakage area A_t and the lateral areas of chamber A_l depend on the geometric profile of the wraps in the central region. If the wraps are considered to be formed just by involutes, these expressions as well as those for the suction area A_s and the flank leakage area A_f can be easily found in the literature. Here, the actual geometry is being taken into account, but the corresponding expressions are omitted due to space limitations.

Due to the shape of the scroll central region, an error arises when one evaluates the volume of the compression chambers by using mathematical relationships available in the literature (Chen *et al.*, 2002; Wang *et al.*, 2005). Such errors can be significant depending on the scroll geometry. In the present study, these volumes were calculated through the integration of parametric functions that define the involute curves of the stationary and the orbiting scrolls vanes, according to Eq. (8). Due to space limitations, the resulting expressions will also not be presented in this paper.

$$V = h\left[\left(\int_{\varphi_{ik,1}}^{\varphi_{ik,2}} y_{i,m}\frac{\mathrm{d}\,x_{i,m}}{\mathrm{d}\,\varphi_i}\mathrm{d}\,\varphi_i - \int_{\varphi_{ok,1}}^{\varphi_{ok,2}} y_{o,f}\frac{\mathrm{d}\,x_{o,f}}{\mathrm{d}\,\varphi_o}\mathrm{d}\,\varphi_o\right) + \left(\int_{\varphi_{ik,1}}^{\varphi_{ik,2}} y_{i,f}\frac{\mathrm{d}\,x_{i,f}}{\mathrm{d}\,\varphi_i}\mathrm{d}\,\varphi_i - \int_{\varphi_{ok,1}}^{\varphi_{ok,2}} y_{o,m}\frac{\mathrm{d}\,x_{o,m}}{\mathrm{d}\,\varphi_o}\mathrm{d}\,\varphi_o\right)\right] \tag{8}$$

The numerical model also takes into account the flow restriction imposed by the orbiting scroll during the discharge process. As can be seen in Fig.1, part of the discharge orifice is blocked by the orbiting scroll. This geometric aspect was included into the model and, hence, only the uncovered area of the discharge orifice (gray area in Fig. 1) is considered during the discharge. Due to the geometrical complexity of the wraps, the uncovered area had to be approximated by mathematical relationships for intersection of circumferences. The result is an expression that is almost exact for the first 1/3 of the discharge process, when flow pressure drops are higher, but overestimates the uncovered area during the remainder of the cycle.

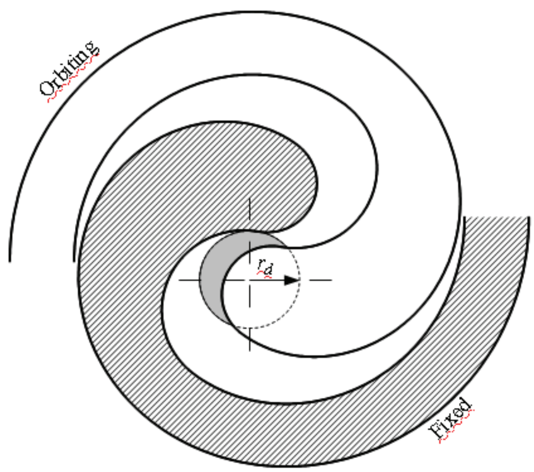

Figure 1: Available flow area during the discharge process.

2.2 Compression Process

The numerical model reported in this paper adopts a lumped formulation and time variations of temperature T, mass m and pressure p in a certain volume of gas are calculated from equations for conservation of mass and energy:

$$\frac{\partial m}{\partial t} = \sum \dot{m}_{in} - \sum \dot{m}_{out} \tag{9}$$

$$\frac{\partial T}{\partial t} = \frac{1}{mc_v}\left\{-T\left(\frac{\partial p}{\partial T}\right)_V\left[\frac{\partial V}{\partial t} - \frac{\left(\sum \dot{m}_{in} - \sum \dot{m}_{out}\right)}{\rho}\right] - \sum \dot{m}_{in}\left(h - h_{in}\right) + \dot{Q}\right\} \tag{10}$$

Equations (9) and (10) are solved by the Euler's method. The third equation required to determine the thermodynamic properties of the gas is an equation of state, which was made available through a link to the library REFPROP (NIST, 2008).

The heat transfer between the gas and the scroll walls $\dot{Q}$ was evaluated by means of a correlation for heat transfer in spiral heat exchangers, proposed by Burmeister (1983) and used in the simulation model of Chen *et al*. (2002):

$$\mathrm{Nu} = 0.023\,\mathrm{Re}^{4/5}\,\mathrm{Pr}^{1/3}\left(1 + 3.5\frac{D_h}{D_c}\right) \tag{11}$$

In Eq. (11), the Reynolds number is based on the hydraulic diameter (D_h = $4V/A_{sup}$) e D_c represents the average diameter of curvature of the wrap D_c [= $A_l/(\pi\, h)$]. It is assumed a linear variation for the scroll wall temperature, with minimum and maximum values depending on the suction and the discharge temperatures.

The mass flow rates associated with the processes of suction, discharge and flank leakage are estimated by the following equation for isentropic flows, corrected by a contraction flow coefficient, C_c:

$$\dot{m} = C_c A \sqrt{2 p_u \rho_u} \sqrt{\frac{\gamma}{\gamma - 1}\left[\left(\frac{p_d}{p_u}\right)^{\frac{2}{\gamma}} - \left(\frac{p_d}{p_u}\right)^{\frac{\gamma+1}{\gamma}}\right]} \tag{12}$$

On the other hand, leakage through the top clearance is predicted by a quasi-1D model, as described by Huang (1994):

$$\frac{\delta^4(\gamma - 1)\mu}{80\gamma p} G^3 + \frac{1}{120}\left(\delta^3 \frac{d\delta}{dx} + \frac{\delta^4}{\gamma p}\frac{dp}{dx}\right) G^2 + \frac{\mu}{\rho} G - \frac{1}{\rho}\frac{dp}{dx} = 0 \tag{13}$$

$$\dot{m} = -\frac{\rho \delta^3}{12} G \tag{14}$$

In Eq. (12), a contraction flow coefficient C_c of 0.7 was adopted for all processes. As the model of Huang (1994) already includes viscous effects and geometric variations, there is no need for specifying a contraction flow coefficient in Eq. (13). In any situation, the pressure ratio is limited by the chocked flow condition:

$$\left(\frac{p_d}{p_u}\right)_{\mathrm{critic}} = \left(\frac{2}{\gamma + 1}\right)^{\frac{\gamma}{\gamma - 1}} \tag{15}$$

The reed is considered to be parallel to the valve seat, with its dynamics being represented by a one-degree-of-freedom model:

$$m_{eq} x + c\,\dot{x} + k\,\ddot{x} = F_p + F_o \tag{16}$$

where m_{eq}, c and k are the reed equivalent mass, damping coefficient and stiffness, respectively. On the other hand, F_p is the force induced by flow on the reed and F_o can accommodate any other force, such as reed pre-tension and also oil stiction. Finally, x, $\dot{x}$ and $\ddot{x}$ are the instantaneous reed lift, velocity and acceleration, respectively. The differential equation for the valve dynamics, Eq. (16), is solved by using an explicit Euler method and by considering the force F_p to be constant during each time step.

Most numerical models are developed to simulate compression in all pockets simultaneously. However, the present model follows a single pocket from the beginning of the suction process to the end of the discharge process. Thus, for the first compression cycle gas properties in the posterior pocket (closer to the central region) are unknown and only the internal gas leakage leaving the pocket is really calculated. During the simulation of a new compression cycle, the mass of gas entering the pocket through leakage is taken from data evaluated in the previous cycle, as outlined in Fig. 2. Besides reducing the complexity of numerical code implementation, this approach also acts as an under-relaxation factor, returning a greater numerical stability for the iterative solution procedure. The convergence of the numerical solution is checked by monitoring the mass unbalance and cyclical variations in the discharge temperature.

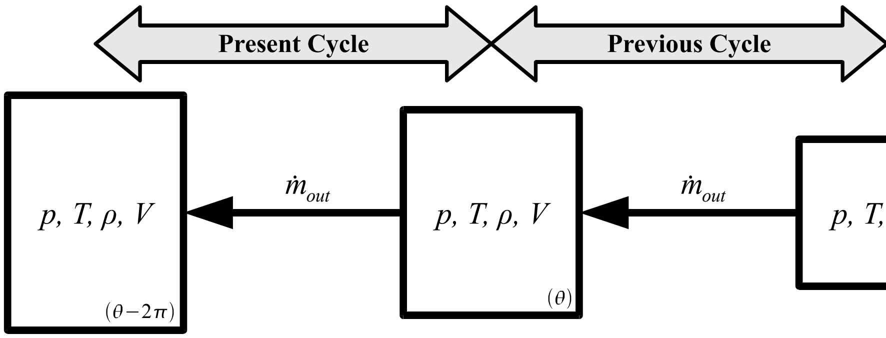

Figure 2: Schematic of the numerical procedure to evaluate internal gas leakages

3. RESULTS AND DISCUSSION

The geometric parameters and the operating conditions used to establish a reference case for the analyses defined in the present study are listed in Tab. 1 and Tab. 2, respectively. A time step equivalent to a crankshaft angle of 0.01º was adopted in all simulations. The solution was admitted to be converged when the cyclical variations of the discharge temperature and the mass unbalance were less than 10^{-2}K and 10^{-6}kg, respectively.

Table 1: Reference geometric parameters

Parameter	Value
Radius of the base circle [mm]	2.0
Wrap thickness [mm]	3.0
Displacement volume [cm³]	2 x 10.0
Number of compression chambers	3
Modified angle [degrees]	20.0
Top clearance [µm]	5.0
Flank clearance [µm]	10.0

Table 2: Reference operating conditions

Parameter	Value
Compressor speed [rpm]	3000.0
Refrigerant fluid	R404a
Evaporating temperature [ºC]	-10.0
Condensing Temperature [ºC]	45.0
Suction Temperature [ºC]	0.0

Initially, the model is used to assess the importance of using a real gas equation of state on the numerical simulation. Figures 3 and 4 present results for pressure and temperature as a function of the pocket volume for two different refrigerant fluids: R404a e R134a. As expected, the ideal gas hypothesis leads to higher pressures and lower gas temperatures. Hence, indicated power is over-predicted and, consequently, compressor efficiency is under-predicted. Naturally, the ideal gas assumption can also deteriorate the prediction of other phenomena. For example, disregarding the effect of leakage, the model with the ideal gas hypothesis predicts a negligible influence of heat transfer on the compressor performance On the other hand, when a real gas equation of state is adopted the model indicates a reduction of almost 4% in the isentropic efficiency, mainly due to differences in the heat transfer process.

By means of a p-V diagram presented in Fig. 5, one can observe the effect of the restriction imposed by the orbiting scroll during the discharge process. At the beginning of the discharge the uncovered area is small, as shown in Fig. 6 and, hence, flow restrictions are high and the chamber pressure rises up. Depending on the geometry of the central part of the wrap, the orbiting scroll can cover part of the orifice throughout the cycle. For the reference geometry adopted in the present analysis, the discharge area increases until the orbiting scroll completely uncovers the orifice, as indicated by the continuous line in Fig. 6. If a modified geometry with a = 1.5mm and γ = 90º is adopted, for example, the uncovered area does not reach 80% of the area made available by the discharge orifice. In this case, at some point, the orbiting scroll starts to cover the orifice again, which becomes completely closed at the end of the discharge process.

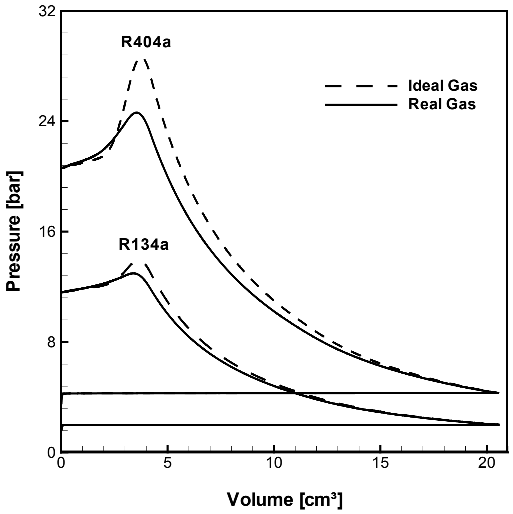

Figure 3. Results for p-V diagram obtained with ideal and real gas hypotheses.

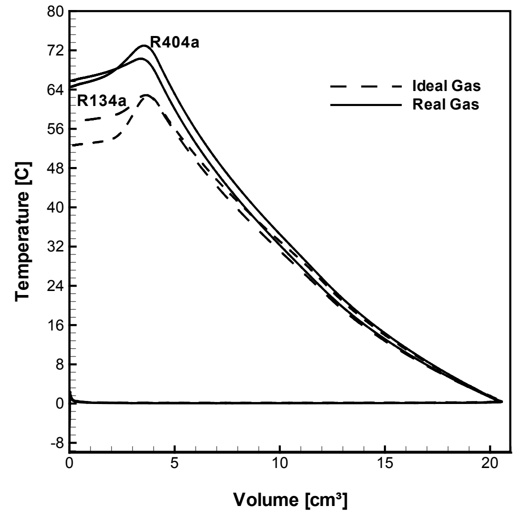

Figure 4. Results for T-V diagram obtained with ideal and real gas hypotheses.

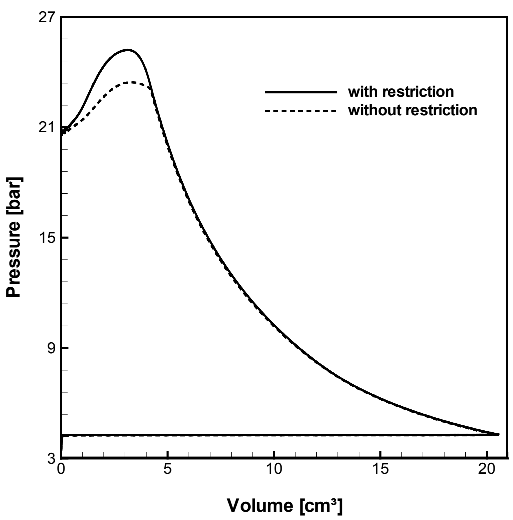

Figure 5. Effect on the p-V diagram due to the flow restriction during the discharge process.

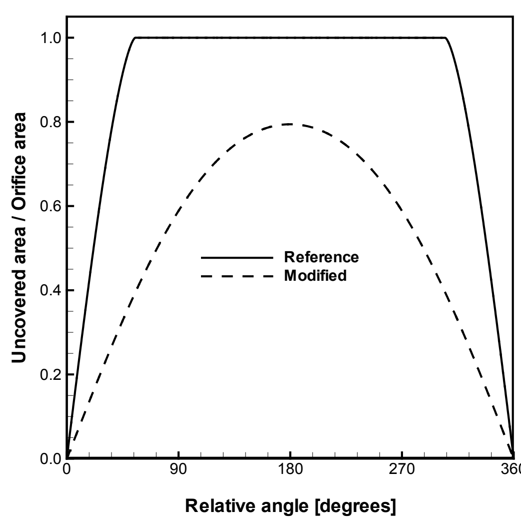

Figure 6. Dimensionless uncovered area for different geometries.

In Fig. 7, the exact volume of a pocket throughout one cycle, described by the integration of Eq. (8), is compared to the volume obtained with the relation presented by Wang *et al*. (2005). Both approaches provide equal volumes up to the crank angle just before the discharge process. After that position, the wraps are not formed exclusively by involutes anymore and the differences become apparent. The main effect of this error in the pocket volume is the under-prediction of the discharge power consumption (Fig. 8), which gives rise to a difference of 1.8% in the isentropic efficiency for this case. It must be observed that such errors are strongly dependent on the scroll geometry and may be negligible in many cases.

In this study it was observed that the solution of the valve dynamics by means of Eq. (16) has not shown advantages over the results provided by a simpler quasi-static model, such as that used by Chen *et al*. (2002), even for higher operation speeds. Nevertheless, when solved by the explicit Euler method, the adoption of Eq. (16) does not require a great computational effort.

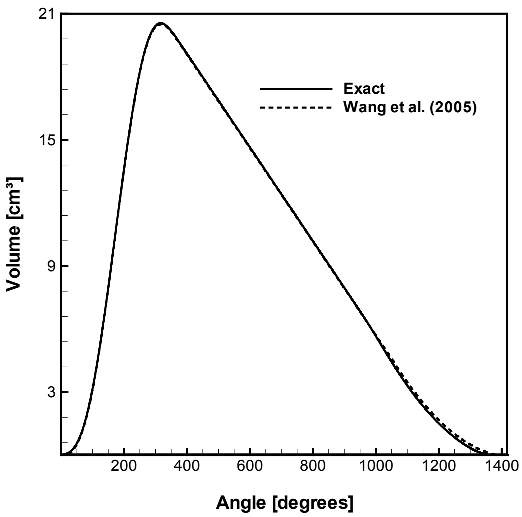

Figure 7. Comparison of pocket volumes obtained by different approaches.

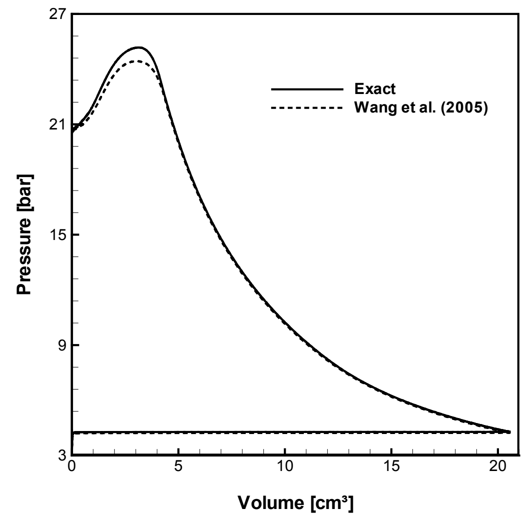

Figure 8. Impact of pocket volume on results for the p-V diagram.

6. CONCLUSIONS

This paper presented a lumped model to simulate the compression process of scroll compressors, with new procedures to evaluate the chamber volumes and to numerically solve the governing equations. Unlike most models proposed in the literature, mathematical expressions are written to accurately evaluate both the volume of the compression chamber and the available valve port area during the discharge process. Additionally, a new solution procedure is devised to simplify the code implementation and to improve the convergence of the iterative procedure. As expected, the real gas equation of state presents a great impact on the numerical predictions and should be used in the compressor modeling. It has been seen that flow restrictions imposed by the orbiting scroll on the discharge process can affect considerably the compressor performance. Even small approximations adopted in the relations to describe the volume of pockets are seen to produce errors of almost 2% in the isentropic efficiency. Finally, it seems that discharge valves can be modeled by a quasi-static approach without any noticeable drawback.

NOMENCLATURE

a	radius of the basic circle [m]
A_f	flank leakage area [m²]
A_l	lateral area of the compression chamber [m²]
A_s	suction area [m²]
A_{sup}	surface area of the chamber [m²]
A_t	top leakage area [m²]
c	damping coefficient of the valve [N.s/m]
C_c	contraction flow coefficient [-]
c_v	specific heat at constant volume [-]
D_c	curvature diameter [m]
D_h	hydraulic diameter [m]
F_o	other force acting on the valve [N]
F_p	gas pressure force on the valve [N]
h	scroll vane height [m]; enthalpy [J/kg/K]
k	stiffness of the valve [N/m]
m	mass [kg]
m_{eq}	equivalent mass of the valve [kg]
$\dot{m}$	mass flow rate [kg/s]
N	number of compression chambers [-]
Nu	Nusselt number [-]
p	pressure [Pa]
Pr	Prandtl number [-]
$\dot{Q}$	heat flow rate into the control volume [W]
r_d	maximum radius of a circular port [m]
Re	Reynolds number [-]
r_o	orbiting radius of the moving scroll [m]
t	scroll vane thickness [m]; time [s]
T	temperature [K]
V_c	volume of chamber [m³]
V_{sw}	displacement volume [m³]
x	valve displacement [m]
$\dot{x}$	valve velocity [m/s]
$\ddot{x}$	valve acceleration [m/s²]
γ	modified angle [rad]; specific heat ratio [-]

δ	gap size [m]	i	inner involute
θ_d	discharge angle [rad]	ik	point of conjugacy on the inner involute
μ	viscosity [Pa.s]	in	entering the control volume
ρ	specific mass [kg/m³]	m	orbiting scroll
φ	involute angle [rad]	o	outer involute
		ok	point of conjugacy on the outer involute
Subscripts		out	leaving the control volume
d	donwstrem	u	upstream
f	fixed scroll		

REFERENCES

ASHRAE, 2004. "Handbook - heating, ventilating and air-conditioning systems and equipment", ASHRAE Inc., Atlanta, USA.

Burmeister, L.C., 1983, "Convective Heat Transfer", Wiley, New York.

Caillat, J.L., Ni, S. and Daniels, M., 1988, "A computer model for scroll compressors", Proc. Int. Compressor Engineering Conference at Purdue University, pp. 47-553.

CARRIER CORPORATION, 2004, "Scroll compressors: high efficiency compression for commercial and industrial applications" New York, USA, 15 Nov. 2008, <http://www.xpedio.carrier.com/idc/groups/public/documents/marketing/811-20065.pdf.>

Chen, Y., Halm, N.P., Groll, E.A. and Braun, J.E, 2002, "Mathematical modeling of scroll compressors – part I: compression process modeling", Int. Journal of Refrigeration 25, pp. 731-750.

Creux, L., 1905, "Rotary Engine", US Patent 801,182.

Ekelöf, J., 1933, "Rotary Pump or Compressor", US Patent 1,906,142.

Gomes, A.R., 2006, "Análise comparativa de mecanismos de compressão para aplicação em refrigeração doméstica", MSc. Thesis – Federal University of Santa Catarina, Department of Mechanical Engineering, in Portuguese.

Huang, Y., 1994, "Leakage calculation through clearances", Proc. Int. Compressor Engineering Conference at Purdue University, pp. 35-40.

Morishita, E., Sugihara, M., Inaba, T., Nakamura, T. and Works, W., 1984, "Scroll compressor analytical model", Proc. Int. Compressor Engineering Conference at Purdue University, pp. 487-495.

Nieter, J.J., 1988, "Dynamics of scroll suction process", Proc. Int. Compressor Engineering Conference at Purdue University, pp. 165-174.

NIST, National Institute of Standards and Technology, 2008, "Refprop - Reference fluid thermodynamic and transport properties", version 8, USA.

Suefuji, K., Shiibayashi, M. and Tojo, K., 1992, "Performance analysis of hermetic scroll compressor", Proc. Int. Compressor Engineering Conference at Purdue University, pp. 75-84.

Tojo, K., Ikegawa, M., Maeda, N., Machida, S., Shiibayashi, M. and Uchikawa, N., 1986, "Computer modeling of scroll compressor with self adjusting back-pressure mechanism", Proc. Int. Compressor Engineering Conference at Purdue University, pp. 872-886.

Wang, B., Li, X., Shi, W., 2005, "A general model of scroll compressors based on discretional initial angles of involute", Int. Journal of Refrigeration, Vol. 28, pp. 958-966.

Yanagisawa, T., Cheng, M.C., Fukuta, M. and Shimizu, T., 1990, "Optimum operating pressure ratio for scroll compressor", Proc. Int. Compressor Engineering Conference at Purdue University, pp. 425-433.

Zhenquan, L., Guirong, D., Shicai, Y., Mingzhi, W., 1992, "The graphic method of modified wrap of scroll compressor", Proc. Int. Compressor Engineering Conference at Purdue University, pp. 1099-1106.

ACKNOWLEDGEMENT

The authors acknowledge the support received from EMBRACO, CNPq (Brazilian Research Council) through Grant No. 573581/2008-8 (National Institute of Science and Technology in Refrigeration and Thermophysics) and FINEP (Federal Agency of Research and Projects Financing).